Boundary element method for a free third boundary problem modeling tumor growth with spectral accuracy

Yarong Zhang, Yinnian He, Hongbin Chen

PII: S0377-0427(18)30384-4
DOI: https://doi.org/10.1016/j.cam.2018.06.032
Reference: CAM 11762

To appear in: *Journal of Computational and Applied Mathematics*

Received date : 14 May 2016
Revised date : 3 May 2018

Please cite this article as: Y. Zhang, Y. He, H. Chen, Boundary element method for a free third boundary problem modeling tumor growth with spectral accuracy, *Journal of Computational and Applied Mathematics* (2018), https://doi.org/10.1016/j.cam.2018.06.032

Boundary element method for a free third boundary problem modeling tumor growth with spectral accuracy ☆

Yarong Zhang[1]*, Yinnian He[1], Hongbin Chen[1]

[1] *Department of Mathematics and Statistics, Xi'an Jiaotong University, Xi'an 710049, P.R. China*

Abstract

By boundary element method, we present a numerical iterative process for solving a free third boundary problem modeling tumor growth with spectral accuracy. The piecewise quadratic curves are fitted to maintain local smoothness of the boundary at every node. The double-layer and single-layer potentials with weakly singular kernels are evaluated with spectral accuracy. The method of characteristics is employed to transform interfacial velocity PDE into discrete ODEs. The numerical integral formula for weakly singular operator with logarithmic singularity is deduced and the convergence and error are presented. The nonradially symmetric solutions of the free boundary problem on a perturbed boundary are provided to test the accuracy and effectiveness of the numerical method.

Keywords: Double-layer and single-layer potentials, characteristic curve, weakly singular kernel, spectral accuracy
2000 MSC: 46E35, 65D05, 65J05

☆This work was supported by the Natural Science Foundations of China (No.11362021), the Major Research and Development Program of China (No. 2016YFB0200901) and the youth project of China's Natural Science Fund (No. 11401045).

*Corresponding author
Email address: yrzhang66@163.com (Yarong Zhang[1])

1. Introduction

In the past thirty years, the theories and numerical methods of the free boundary problems [1, 2, 3, 4, 5, 6, 7, 8, 9] have been studied extensively. Due to the changing domain and the moving boundary, it is difficult to analyze theoretically or solve numerically the free boundary problems, and the numerical methods always need the large scale numerical computations. In recent years, different kinds approximation techniques have been developed and carried out to get numerical solutions with minimal possible errors for the free boundary problems, among them boundary element method [10, 11, 12, 13] is the most efficient and accurate method because the dimensionality of the problem is cutted down by one. The boundary integral equations are only solved at the moving boundary, thus the number of unknowns is dramatically reduced.

However, the accuracy of the boundary element method depends on the order of the elements and the accuracy of the numerical integration. Even though the quadratic elements commonly used in practice lead to at most second order accuracy in space [14]. Thanks to the editor and the reviwers whose comments brought us to Nystrom's method [15, 16] and Hilbert transform to compute the singular integrals with spectral accuracy(see[14, 15, 16, 17, 18]). In this paper, we successfully adopt these quadrature methods to the free boundary problem modeling tumor growth and achieve spectral accuracy.

It is worthy of noting that the spectral accuracy is hard to achieve because of geometric discontinuity at the edges of the elements [14]. On the basis of Hermitian-like interpolations, a appropriate boundary smoothing technique was adopted to maintain the continuity of the boundary at the edges of the elements by Dimitrakopoulos and Wang [18]. Also, Sun and Li [14], Kropinski [19] employed Fourier series to represent the boundary and make better the spatial accuracy. In this paper, we fit the piecewise quadratic curve at each node by this node and its two adjacent nodes, and all the computational nodes of the tumor boundary are covered twice by the piecewise quadratic curves so that there is a local quadratic curve smoothly passing through each node, which can keep the local smoothness of the boundary curve and the existence of until infinity derivative at each node. In fact, we always use this piecewise quadratic curve and its until the second derivative at each node in our numerical computations such as (3.31), (3.32), (3.35), (3.37) and so on.

In this paper, we consider a tumor mathematical model with the free nonhomogeneous boundary conditions of the third kind. Boundary element

method is implemented to solve this model with spectral accuracy. We adopt a new interfacial smoothing technique described in the above paragraph to maintain the local smoothness of the boundary at each node, and the higher order orthogonal polynomials are employed to analyze and evaluate the singular single-layer and double-layer potentials, which result in a more efficient simulation process and successfully achieve spectral accuracy. Additionally, our numerical simulations help to predict the expansion or contraction of the tumor volume in clinical medicine which primarily come from reproduction or death of tumor cells respectively, and reveal the affect of each relevant parameter to tumour evolution.

The organization of this work is as follows: in section 2, the governing equations are presented. In section 3, the single-layer and double-layer potentials with weakly singular kernels are analyzed and evaluated with spectral accuracy, and the numerical schemes of the free boundary integral equations are derived. In Section 4, the characteristic curve method is applied to transform interfacial velocity PDE into discrete ODEs. In section 5, the numerical integral formula with weakly singular kernel is deduced and the convergence and error for such approximation schemes are presented. In section 6, Example is provided to demonstrate the accuracy and effectiveness of the numerical method. In section 7, the conclusions are given.

2. A Free Third Boundary Problem Modeling Tumor Growth

$\Omega(t)$ denotes the tumor domain at time t and $\Gamma(t)$ is the boundary of $\Omega(t)$. Modeling the tumor as an incompressible fluid, it is reasonable to assume that the velocity field $\vec{v}(\mathbf{x},t)$ in $\Omega(t)$ satisfies Darcy's law $\vec{v} = -\nabla p$ and the law of conservation of mass $\mathrm{div}\vec{v} = \mu(\sigma - \tilde{\sigma})$. Where $p(\mathbf{x},t)$ is the pressure within the tumor results from proliferation of the tumor cells, $\sigma(\mathbf{x},t)$ is the modified nutrient concentration of the tumor, μ is the proliferation rate which expresses the ?intensity? of the expansion or shrinkage, and $\widetilde{\sigma} > 0$ is a threshold concentration of nutrients needed for sustainability.

Then we can deduce directly that

$$\mathrm{div}\vec{v} = \mathrm{div}(-\nabla p) = -\Delta p = \mu(\sigma - \tilde{\sigma}), \qquad \mathbf{x} \in \Omega(t). \tag{2.1}$$

and the normal velocity v_n of $\Gamma(t)$ in the outward normal direction $\overrightarrow{n}$

$$\vec{v} \cdot \overrightarrow{n} = -\nabla p \cdot \overrightarrow{n}, \qquad \mathbf{x} \in \Gamma(t),$$

i.e.,

$$v_n(\mathbf{x},t) = -\frac{\partial p(\mathbf{x},t)}{\partial n}, \qquad \mathbf{x} \in \Gamma(t).$$

In this paper, we consider the free boundary problem modeling tumor growth with the boundary conditions of the third kind as follows

$$\begin{cases} \lambda\sigma_t - \Delta\sigma(\mathbf{x},t) + \sigma(\mathbf{x},t) &= 0, & \mathbf{x} \in \Omega(t), \\ -\Delta p(\mathbf{x},t) &= \mu(\sigma(\mathbf{x},t) - \widetilde{\sigma}), & \mathbf{x} \in \Omega(t), \\ \sigma(\mathbf{x},t) + \frac{\partial\sigma(\mathbf{x},t)}{\partial n} &= 1 & \mathbf{x} \in \Gamma(t), \\ p(\mathbf{x},t) + \frac{\partial p(\mathbf{x},t)}{\partial n} &= \kappa(\mathbf{x},t) & \mathbf{x} \in \Gamma(t), \\ \frac{\partial p(\mathbf{x},t)}{\partial n} &= -v_n(\mathbf{x},t) & \mathbf{x} \in \Gamma(t). \end{cases} \tag{2.2}$$

Because λ is small, one can set $\lambda = 0$. Substituting $\sigma(\mathbf{x},t) = \Delta\sigma(\mathbf{x},t)$ into $-\Delta p(\mathbf{x},t) = \mu(\sigma(\mathbf{x},t) - \widetilde{\sigma})$, then, $-\Delta p(\mathbf{x},t) = \mu(\sigma(\mathbf{x},t) - \widetilde{\sigma})$ can be rewrited as

$$-\Delta[p(\mathbf{x},t) + \mu(\sigma(\mathbf{x},t) - \widetilde{\sigma}\frac{|\mathbf{x}|^2}{2d})] = 0, \ \mathbf{x} \in \Omega(t),$$

noting that $\Delta|\mathbf{x}|^2 = 2d$ and d is the dimension.

$P(\mathbf{x},t) \triangleq p(\mathbf{x},t) + \mu(\sigma(\mathbf{x},t) - \widetilde{\sigma}\frac{|\mathbf{x}|^2}{2d})$, we get

$$-\Delta P(\mathbf{x},t) = 0, \ \mathbf{x} \in \Omega(t).$$

Then, the free boundary problem (2.2) can be rewritten as

$$\begin{cases} -\Delta\sigma(\mathbf{x},t) + \sigma(\mathbf{x},t) &= 0 & \mathbf{x} \in \Omega(t), \\ -\Delta P(\mathbf{x},t) &= 0 & \mathbf{x} \in \Omega(t). \\ \sigma(\mathbf{x},t) + \frac{\partial\sigma(\mathbf{x},t)}{\partial n} &= 1 & \mathbf{x} \in \Gamma(t), \\ P(\mathbf{x},t) + \frac{\partial P(\mathbf{x},t)}{\partial n} &= \kappa(\mathbf{x},t) + \mu[1 - \frac{\widetilde{\sigma}}{2d}(|\mathbf{x}|^2 + \frac{\partial|\mathbf{x}|^2}{\partial n})], & \mathbf{x} \in \Gamma(t) \\ \frac{\partial P(\mathbf{x},t)}{\partial n} &= -v_n(\mathbf{x},t) + \mu[\frac{\partial\sigma(\mathbf{x},t)}{\partial n} - \frac{\widetilde{\sigma}}{2d}\frac{\partial|\mathbf{x}|^2}{\partial n}], & \mathbf{x} \in \Gamma(t), \end{cases} \tag{2.3}$$

where κ denotes the mean curvature.

The Helmholtz and Laplace equations in problem (2.3) can be transformed into the following boundary integral equations, respectively,

$$\frac{\sigma(\mathbf{x})}{2} = \int_{\partial\Omega}\left[G_1(\mathbf{x},\mathbf{y})\frac{\partial\sigma(\mathbf{y})}{\partial n} - \sigma(\mathbf{y})\frac{\partial G_1(\mathbf{x},\mathbf{y})}{\partial n}\right]dS_{\mathbf{y}}, \quad \mathbf{x} \in \Gamma(t), \tag{2.4}$$

$$\frac{P(\mathbf{x})}{2} = \int_{\partial\Omega} \left[G_2(\mathbf{x},\mathbf{y}) \frac{\partial P(\mathbf{y})}{\partial n} - P(\mathbf{y}) \frac{\partial G_2(\mathbf{x},\mathbf{y})}{\partial n} \right] dS_{\mathbf{y}}, \quad \mathbf{x} \in \Gamma(t), \qquad (2.5)$$

where G_1 and G_2 are the Green functions corresponding to the operator $-\Delta+1$ and $-\Delta$, separately. For three dimensional case, $G_1(\mathbf{x},\mathbf{y}) = \frac{1}{4\pi}\frac{e^{-|\mathbf{x}-\mathbf{y}|}}{|\mathbf{x}-\mathbf{y}|}$, $G_2(\mathbf{x},\mathbf{y}) = \frac{1}{4\pi|\mathbf{x}-\mathbf{y}|}$. For two dimensional case, $G_1(\mathbf{x},\mathbf{y}) = \frac{i}{4}H_0^{(1)}(i|\mathbf{x}-\mathbf{y}|)$, $G_2(\mathbf{x},\mathbf{y}) = -\frac{1}{2\pi} ln(|\mathbf{x}-\mathbf{y}|)$, $H_0^{(1)}$ is a Hankel function.

Substituting the boundary condition $\sigma(\mathbf{x},t) + \frac{\partial\sigma(\mathbf{x},t)}{\partial n} = 1$ into (2.4), we obtain

$$\frac{\sigma(\mathbf{x})}{2} = \int_{\partial\Omega} \left[G_1(\mathbf{x},\mathbf{y})(1-\sigma(\mathbf{y})) - \sigma(\mathbf{y}) \frac{\partial G_1(\mathbf{x},\mathbf{y})}{\partial n} \right] dS_{\mathbf{y}}, \quad \mathbf{x} \in \Gamma(t),$$

i.e.,

$$\frac{\sigma(\mathbf{x})}{2} + \int_{\partial\Omega} \sigma(\mathbf{y}) \left[G_1(\mathbf{x},\mathbf{y}) + \frac{\partial G_1(\mathbf{x},\mathbf{y})}{\partial n} \right] dS_{\mathbf{y}} = \int_{\partial\Omega} G_1(\mathbf{x},\mathbf{y}) dS_{\mathbf{y}}, \quad \mathbf{x} \in \Gamma(t). \qquad (2.6)$$

Substituting the boundary condition $P + \frac{\partial P(\mathbf{x},t)}{\partial n} = \kappa(\mathbf{x},t) + \mu[1 - \frac{\widetilde{\sigma}}{2d}(|\mathbf{x}|^2 + \frac{\partial|\mathbf{x}|^2}{\partial n})]$ into (2.5), we have

$$\frac{P(\mathbf{x})}{2} = \int_{\partial\Omega} \left\{ G_2(\mathbf{x},\mathbf{y}) \left[\kappa(\mathbf{y},t) + \mu[1 - \frac{\widetilde{\sigma}}{2d}(|\mathbf{y}|^2 + \frac{\partial|\mathbf{y}|^2}{\partial n})] - P(\mathbf{y}) \right] - P(\mathbf{y}) \frac{\partial G_2(\mathbf{x},\mathbf{y})}{\partial n} \right\} dS_{\mathbf{y}}, \quad \mathbf{x} \in \Gamma(t),$$

i.e.,

$$\begin{aligned} &\frac{P(\mathbf{x})}{2} + \int_{\partial\Omega} P(\mathbf{y}) \left[G_2(\mathbf{x},\mathbf{y}) + \frac{\partial G_2(\mathbf{x},\mathbf{y})}{\partial n} \right] dS_{\mathbf{y}} \\ = &\int_{\partial\Omega} G_2(\mathbf{x},\mathbf{y}) \left\{ \kappa(\mathbf{y},t) + \mu[1 - \frac{\widetilde{\sigma}}{2d}(|\mathbf{y}|^2 + \frac{\partial|\mathbf{y}|^2}{\partial n})] \right\} dS_{\mathbf{y}}, \quad \mathbf{x} \in \Gamma(t). \end{aligned} \qquad (2.7)$$

On the one hand, the boundary integral equations (2.6) and (2.7) reduce the dimensionality of the problem (2.3) by one, so computational cost is reduced dramatically.

On the other hand, the boundary integral equations (2.6) and (2.7) involve double-layer and single-layer potentials with weakly singular kernels, and $\sigma(\mathbf{x})$, $P(\mathbf{x})$ as the unknown, respectively. We will subtract the logarithmic singularity from these integrals in R^2, and spectral accuracy will be derived.

3. Single-layer and Double-layer Potentials with Weakly Singular Kernels are Analyzed and Evaluated

In this section, we design the numerical schemes for the boundary integral equations (2.6) and (2.7) which contain the logarithmic singularities in two-dimensional space.

We use the polar coordinate system. Assuming tumor domains are star shapes without large deformations (if not, one can take $ds = \frac{L}{2\pi}d\theta$, where L is the length of the tumor boundary), we decompose the interval $[0, 2\pi]$ of polar angle θ with uniform grid points $0 = \theta_0 < \theta_1 < ... < \theta_{k-1} < \theta_k < \theta_{k+1} < ... < \theta_N = 2\pi$.

In order to maintain the local smoothness of the boundary at the edges of the elements, we fit the boundary of the tumor by the piecewise quadratic curve

$$r_k(\theta) = a_k(\theta - k\Delta\theta)^2 + b_k(\theta - k\Delta\theta) + c_k, k = 1, 2, 3, ..., 2n, \tag{3.1}$$

in the interval $[\theta_{k-1}, \theta_{k+1}]$ at each node, where $\Delta\theta = \frac{2\pi}{2n}$. We can determine a_k, b_k, c_k by three points $(r((k-1)\Delta\theta), (k-1)\Delta\theta)$, $(r(k\Delta\theta), k\Delta\theta)$ and $(r((k+1)\Delta\theta), (k+1)\Delta\theta)$, $k = 1, 2, 3, ..., 2n$, where $r(\theta_{2n}) = r(\theta_0)$ and $r(\theta_{2n+1}) = r(\theta_1)$.

From (3.1), we infer

$$r_k'(\theta) = 2a_k(\theta - k\Delta\theta) + b_k, k = 1, 2, 3, ..., 2n \tag{3.2}$$

$$r_k''(\theta) = 2a_k, k = 1, 2, 3, ..., 2n \tag{3.3}$$

and

$$r_k(k\Delta\theta) = c_k, r_k'(k\Delta\theta) = b_k, r_k''(k\Delta\theta) = 2a_k, k = 1, 2, 3, ..., 2n. \tag{3.4}$$

For convenience, $r_k(\theta)$ is denoted by $r(\theta)$ in this paper.

Firstly, we consider the boundary integral equations (2.6)

$$\sigma(\mathbf{x}) + 2\int_{\partial\Omega}\sigma(\mathbf{y})\left[G_1(\mathbf{x},\mathbf{y}) + \frac{\partial G_1(\mathbf{x},\mathbf{y})}{\partial n}\right]dS_{\mathbf{y}} = 2\int_{\partial\Omega}G_1(\mathbf{x},\mathbf{y})dS_{\mathbf{y}}, \quad \mathbf{x}\in\Gamma(t), \tag{3.5}$$

where $G_1(\mathbf{x},\mathbf{y}) = \frac{i}{4}H_0^{(1)}(i|\mathbf{x}-\mathbf{y}|)$, $\mathbf{x} = \big(\overline{x},\overline{y}\big) = r(\overline{\theta})\big(\cos\overline{\theta},\sin\overline{\theta}\big)$, $\mathbf{y} = \big(x,y\big) = r(\theta)\big(\cos\theta,\sin\theta\big)$ and

$$|\mathbf{x}-\mathbf{y}| = \sqrt{(x-\overline{x})^2 + (y-\overline{y})^2}$$

$$= \sqrt{r^2(\theta) - 2r(\theta)r(\overline{\theta})\cos(\theta - \overline{\theta}) + r^2(\overline{\theta})}. \qquad (3.6)$$

Hence, the left side of (3.5) is calculated as

$$\begin{aligned}
&\sigma(\mathbf{x}) + 2\int_{\partial\Omega} \sigma(\mathbf{y}) \left[G_1(\mathbf{x},\mathbf{y}) + \frac{\partial G_1(\mathbf{x},\mathbf{y})}{\partial n} \right] dS_{\mathbf{y}} \\
= \;& \sigma(\mathbf{x}) + \frac{i}{2}\int_{\partial\Omega} \sigma(\mathbf{y}) \left[H_0^{(1)}(i|\mathbf{x}-\mathbf{y}|) + \nabla H_0^{(1)}(i|\mathbf{x}-\mathbf{y}|)\cdot \overrightarrow{n} \right] dS_{\mathbf{y}} \\
= \;& \sigma(\overline{\theta}) + \frac{1}{2}\int_0^{2\pi} \sigma(\theta) \Big[iH_0^{(1)}(i\sqrt{r^2(\theta) - 2r(\theta)r(\overline{\theta})\cos(\theta-\overline{\theta}) + r^2(\overline{\theta})})\sqrt{r^2(\theta) + r'^2(\theta)} \\
&+ \frac{H_1^{(1)}(i\sqrt{r^2(\theta) + r^2(\overline{\theta}) - 2r(\theta)r(\overline{\theta})\cos(\theta-\overline{\theta})})}{\sqrt{r^2(\theta) + r^2(\overline{\theta}) - 2r(\theta)r(\overline{\theta})\cos(\theta-\overline{\theta})}} (r^2(\theta) - r(\theta)r(\overline{\theta})\cos(\theta-\overline{\theta}) \\
&+ r'(\theta)r(\overline{\theta})\sin(\overline{\theta}-\theta)) \Big] d\theta, \qquad (3.7)
\end{aligned}$$

where

$$dS_{\mathbf{y}} = \sqrt{(x'(\theta))^2 + (y'(\theta))^2}\, d\theta = \sqrt{r^2(\theta) + r'^2(\theta)}\, d\theta.$$

The right side of (3.5) is specified as

$$\begin{aligned}
&2\int_{\partial\Omega} G_1(\mathbf{x},\mathbf{y}) dS_{\mathbf{y}} = \frac{i}{2}\int_{\partial\Omega} H_0^{(1)}(i|\mathbf{x}-\mathbf{y}|) dS_{\mathbf{y}} \\
= \;& \frac{i}{2}\int_0^{2\pi} H_0^{(1)}(i\sqrt{r^2(\theta) - 2r(\theta)r(\overline{\theta})\cos(\theta-\overline{\theta}) + r^2(\overline{\theta})})\sqrt{r^2(\theta) + r'^2(\theta)}\, d\theta. \qquad (3.8)
\end{aligned}$$

Combining (3.7) and (3.8), we get

$$\begin{aligned}
&\sigma(\overline{\theta}) + \frac{1}{2}\int_0^{2\pi} \sigma(\theta) \Big[iH_0^{(1)}(i\sqrt{r^2(\theta) - 2r(\theta)r(\overline{\theta})\cos(\theta-\overline{\theta}) + r^2(\overline{\theta})})\sqrt{r^2(\theta) + r'^2(\theta)} \\
&+ \frac{H_1^{(1)}(i\sqrt{r^2(\theta) + r^2(\overline{\theta}) - 2r(\theta)r(\overline{\theta})\cos(\theta-\overline{\theta})})}{\sqrt{r^2(\theta) + r^2(\overline{\theta}) - 2r(\theta)r(\overline{\theta})\cos(\theta-\overline{\theta})}} (r^2(\theta) - r(\theta)r(\overline{\theta})\cos(\theta-\overline{\theta}) \\
&+ r'(\theta)r(\overline{\theta})\sin(\overline{\theta}-\theta)) \Big] d\theta \\
= \;& \frac{i}{2}\int_0^{2\pi} H_0^{(1)}(i\sqrt{r^2(\theta) - 2r(\theta)r(\overline{\theta})\cos(\theta-\overline{\theta}) + r^2(\overline{\theta})})\sqrt{r^2(\theta) + r'^2(\theta)}\, d\theta. \qquad (3.9)
\end{aligned}$$

For simplicity, we confine ourselves to a special case $r(\theta) = 1$. It follows from (3.9)

$$\sigma(\overline{\theta}) + \frac{1}{2}\int_0^{2\pi} \sigma(\theta)\Big[iH_0^{(1)}(i\sqrt{2(1-\cos(\theta-\overline{\theta}))} + \frac{H_1^{(1)}(i\sqrt{2(1-\cos(\theta-\overline{\theta}))})}{\sqrt{2(1-\cos(\theta-\overline{\theta})}}$$
$$\cdot(1-\cos(\theta-\overline{\theta}))\Big]d\theta = \frac{i}{2}\int_0^{2\pi} H_0^{(1)}(i\sqrt{2(1-\cos(\theta-\overline{\theta}))})d\theta, \tag{3.10}$$

i.e.,

$$\sigma(\overline{\theta}) + \frac{1}{2\pi}\int_0^{2\pi} \pi\cdot\sigma(\theta)\Big[iH_0^{(1)}(2i|sin\frac{\theta-\overline{\theta}}{2}|) + |sin\frac{\theta-\overline{\theta}}{2}|\cdot H_1^{(1)}(2i|sin\frac{\theta-\overline{\theta}}{2}|)\Big]d\theta$$
$$= \frac{1}{2\pi}\int_0^{2\pi} \pi i\cdot H_0^{(1)}(2i|sin\frac{\theta-\overline{\theta}}{2}|)d\theta. \tag{3.11}$$

The Hankel function H_0^1 can be decomposed by

$$H_0^1 = J_0 + iY_0, \tag{3.12}$$

where

$$J_0(z) = \sum_{k=0}^{\infty}\frac{(-1)^k}{(k!)^2}(\frac{z}{2})^{2k} \tag{3.13}$$

and

$$Y_0(z) = \frac{2}{\pi}(ln\frac{z}{2}+b)J_0(z) - \frac{2}{\pi}\sum_{k=0}^{\infty} a_k\frac{(-1)^k}{(k!)^2}(\frac{z}{2})^{2k}, \tag{3.14}$$

with $a_k = \sum_{m=1}^{k}\frac{1}{m}$, $b = 0.57721...$

Additionally, $(H_0^1)' = -H_1^1$, $H_1^1 = J_1 + iY_1$.

We rewrite (3.11) as

$$\sigma(\overline{\theta}) + \frac{1}{2\pi}\int_0^{2\pi}\sigma(\theta)\Big[K(\theta,\overline{\theta}) + M(\theta,\overline{\theta})\Big]d\theta$$
$$= \frac{1}{2\pi}\int_0^{2\pi} K(\theta,\overline{\theta})d\theta \tag{3.15}$$

Using (3.12), (3.13) and (3.14), we split off the singular kernel

$$K(\theta,\overline{\theta}) = \pi i \cdot H_0^{(1)}(2i|sin\frac{\theta-\overline{\theta}}{2}|) = \pi i \cdot J_0(2i|sin\frac{\theta-\overline{\theta}}{2}|) - \pi Y_0(2i|sin\frac{\theta-\overline{\theta}}{2}|)$$

$$\begin{aligned} &= \pi i \cdot J_0(2i|sin\frac{\theta-\overline{\theta}}{2}|) + [-2ln(i|sin\frac{\theta-\overline{\theta}}{2}|) - 2C]J_0(2i|sin\frac{\theta-\overline{\theta}}{2}|) \\ &\quad +2\sum_{k=0}^{\infty} a_k \frac{(-1)^k}{(k!)^2}(i|sin\frac{\theta-\overline{\theta}}{2}|)^{2k} \\ &= [-ln(4sin^2\frac{\theta-\overline{\theta}}{2}) - 2lni + ln4 - 2C]J_0(2i|sin\frac{\theta-\overline{\theta}}{2}|) + \pi i \cdot J_0(2i|sin\frac{\theta-\overline{\theta}}{2}|) \\ &\quad +2\sum_{k=0}^{\infty} a_k \frac{(-1)^k}{(k!)^2}(i|sin\frac{\theta-\overline{\theta}}{2}|)^{2k} \\ &\triangleq K_1(\theta,\overline{\theta})ln(4sin^2\frac{\theta-\overline{\theta}}{2}) + K_2(\theta,\overline{\theta}), \end{aligned} \tag{3.16}$$

where

$$K_1(\theta,\overline{\theta}) = -J_0(2i|sin\frac{\theta-\overline{\theta}}{2}|), \tag{3.17}$$

and

$$\begin{aligned} K_2(\theta,\overline{\theta}) &= (-2lni + ln4 - 2C)J_0(2i|sin\frac{\theta-\overline{\theta}}{2}|) + \pi i \cdot J_0(2i|sin\frac{\theta-\overline{\theta}}{2}|) \\ &\quad +2\sum_{k=0}^{\infty} a_k \frac{(-1)^k}{(k!)^2}(i|sin\frac{\theta-\overline{\theta}}{2}|)^{2k} \\ &= K(\theta,\overline{\theta}) - K_1(\theta,\overline{\theta})ln(4sin^2\frac{\theta-\overline{\theta}}{2}), \end{aligned} \tag{3.18}$$

noting that K_1 and K_2 are analytic. $K_2(\theta,\theta) = -2ln\frac{i}{2} + i\pi - 2C$.

Similarly, we can decompose the singular kernel

$$\begin{aligned} M(\theta,\overline{\theta}) &= \pi \cdot |sin\frac{\theta-\overline{\theta}}{2}| \cdot H_1^{(1)}(2i|sin\frac{\theta-\overline{\theta}}{2}|) \\ &= M_1(\theta,\overline{\theta})ln(4sin^2\frac{\theta-\overline{\theta}}{2}) + M_2(\theta,\overline{\theta}), \end{aligned} \tag{3.19}$$

where

$$M_1(\theta,\overline{\theta}) = i \cdot sin\frac{\theta-\overline{\theta}}{2} \cdot J_1(2isin\frac{\theta-\overline{\theta}}{2}), \tag{3.20}$$

$$M_2(\theta,\overline{\theta}) = M(\theta,\overline{\theta}) - M_1(\theta,\overline{\theta})ln(4sin^2\frac{\theta-\overline{\theta}}{2}), \tag{3.21}$$

and M_1 and M_2 are analytic. $M_2(\theta,\theta) = 1$.

Furthermore, (3.15) can be rewrited by

$$\sigma(\overline{\theta}) + \frac{1}{2\pi}\int_0^{2\pi}\sigma(\theta)\Big[K_1(\theta,\overline{\theta})ln(4sin^2\frac{\theta-\overline{\theta}}{2}) + K_2(\theta,\overline{\theta}) + M_1(\theta,\overline{\theta})ln(4sin^2\frac{\theta-\overline{\theta}}{2})$$
$$+M_2(\theta,\overline{\theta})\Big]d\theta = \frac{1}{2\pi}\int_0^{2\pi}[K_1(\theta,\overline{\theta})ln(4sin^2\frac{\theta-\overline{\theta}}{2}) + K_2(\theta,\overline{\theta})]d\theta. \tag{3.22}$$

For an analytic and periodic function K_1, we have the following quadrature formula

$$\frac{1}{2\pi}\int_0^{2\pi}K_1(\theta,\theta_j)ln(4sin^2\frac{\theta-\theta_j}{2})d\theta \approx \sum_{k=0}^{2n-1}R_j^n(\theta_k)K_1(\theta_j,\theta_k), j = 0,1,2,...,2n-1, \tag{3.23}$$

with the quadrature weights

$$R_j^n(\theta_k) = -\frac{1}{n}\{\sum_{m=1}^{n-1}\frac{1}{m}cosm(\theta_k-\theta_j) + \frac{1}{2n}cosn(\theta_k-\theta_j)\}, \quad j = 0,1,2,...,2n-1. \tag{3.24}$$

For the integral involving the kernel K_2, we use the composite trapezoidal rule

$$\frac{1}{2\pi}\int_0^{2\pi}K_2(\theta,\theta_j)d\theta \approx \frac{1}{2n}\sum_{k=0}^{2n-1}K_2(\theta_j,\theta_k), \quad j = 0,1,2,...,2n-1. \tag{3.25}$$

The other items are the same as (3.23) and (3.25), we then approximate the singular integral equation (3.22) by a finite-dimensional linear system

$$\sigma(\theta_{\mathbf{j}}) + \sum_{k=0}^{2n-1}\sigma(\theta_{\mathbf{k}})\Big[R_j^n(\theta_k)K_1(\theta_j,\theta_k) + \frac{1}{2n}K_2(\theta_j,\theta_k) + R_j^n(\theta_k)M_1(\theta_j,\theta_k) + \frac{1}{2n}M_2(\theta_j,\theta_k)\Big]$$
$$= \sum_{k=0}^{2n-1}[R_j^n(\theta_k)K_1(\theta_j,\theta_k) + \frac{1}{2n}K_2(\theta_j,\theta_k)], \qquad j = 0,1,2,...,2n-1, \tag{3.26}$$

with the quadrature weights

$$R_j^n(\theta_k) = -\frac{1}{n}\{\sum_{m=1}^{n-1}\frac{1}{m}cosm(\theta_k-\theta_j) + \frac{1}{2n}cosn(\theta_k-\theta_j)\}, \quad j = 0,1,2,...,2n-1. \tag{3.27}$$

In particularly, for evenly spaced nodes, $\theta_k = \frac{2\pi k}{2n}$, $\theta_j = \frac{2\pi j}{2n}$, the quadrature weights (3.24) of the formula (3.23) can be simplified as

$$\begin{aligned} R_j^n(\theta_k) &= -\frac{1}{n}\{\sum_{m=1}^{n-1}\frac{1}{m}cos\frac{m\pi(k-j)}{n} + \frac{1}{2n}cos\pi(k-j)\} \\ &= -\frac{1}{n}\{\sum_{m=1}^{n-1}\frac{1}{m}cos\frac{m\pi(k-j)}{n} + \frac{(-1)^{(k-j)}}{2n}\} \triangleq R_{k-j}^{(n)}, \\ & \qquad k,j = 0,1,2,...,2n-1. \end{aligned} \tag{3.28}$$

and the quadrature formula (3.23) yields spectral accuracy.

Now, we turn our attention to the singular boundary integral equation (2.7),

$$\begin{aligned} & P(\mathbf{x}) + 2\int_{\partial\Omega} P(\mathbf{y})\left[G_2(\mathbf{x},\mathbf{y}) + \frac{\partial G_2(\mathbf{x},\mathbf{y})}{\partial n}\right]dS_{\mathbf{y}} \\ = \; & 2\int_{\partial\Omega} G_2(\mathbf{x},\mathbf{y})\left\{\kappa(\mathbf{y}) + \mu[1 - \frac{\widetilde{\sigma}}{2d}(|\mathbf{y}|^2 + \frac{\partial|\mathbf{y}|^2}{\partial n})]\right\}dS_{\mathbf{y}}, \quad \mathbf{x}\in\Gamma(t), \end{aligned} \tag{3.29}$$

where $G_2(\mathbf{x},\mathbf{y}) = -\frac{1}{2\pi}ln(|\mathbf{x}-\mathbf{y}|)$.

For the double-layer potential, we have

$$2\int_{\partial\Omega} P(\mathbf{y})\frac{\partial G_2(\mathbf{x},\mathbf{y})}{\partial n}dS_{\mathbf{y}} = -\int_0^{2\pi} P(\theta)N(\theta,\overline{\theta})d\theta, \tag{3.30}$$

where

$$N(\theta,\overline{\theta}) = \frac{1}{\pi}\frac{r^2(\theta) - r(\theta)r(\overline{\theta})\cos(\theta-\overline{\theta}) + r^{'}(\theta)r(\overline{\theta})\sin(\overline{\theta}-\theta)}{r^2(\theta) + r^2(\overline{\theta}) - 2r(\theta)r(\overline{\theta})\cos(\theta-\overline{\theta})}, \quad \theta\neq\overline{\theta}, \tag{3.31}$$

$$N(\theta,\overline{\theta}) = \frac{1}{2\pi}\frac{r(\theta)r^{''}(\theta) - r^2(\theta) - 2(r^{'}(\theta))^2}{r^2(\theta) + r'^2(\theta)}, \quad \theta=\overline{\theta}, \tag{3.32}$$

and the kernel $N(\theta,\overline{\theta})$ is continuous provided Γ is of class C^2.

For the single-layer potential, we have

$$2\int_{\partial\Omega} P(\mathbf{y})G_2(\mathbf{x},\mathbf{y})dS_{\mathbf{y}} = \frac{1}{4\pi}\int_0^{2\pi} P(\theta)[-ln(4sin^2\frac{\theta-\overline{\theta}}{2}) + Q(\theta,\overline{\theta})]d\theta, \tag{3.33}$$

with

$$Q(\theta,\overline{\theta}) = ln\frac{4sin^2\frac{\theta-\overline{\theta}}{2}}{r^2(\theta)+r^2(\overline{\theta})-2r(\theta)r(\overline{\theta})\cos(\theta-\overline{\theta})} - \frac{1}{|\Gamma|}$$
$$\cdot\int_0^{2\pi} ln\frac{1}{r^2(\theta)+r^2(\overline{\theta})-2r(\theta)r(\overline{\theta})\cos(\theta-\overline{\theta})}\sqrt{r^2(\theta)+r'^2(\theta)}d\theta + \frac{4\pi}{|\Gamma|}, \quad \theta\neq\overline{\theta}, \quad (3.34)$$

and Q is continuously differentiable provided Γ is of class C^2.

Employing the same computational strategy and combining (3.30) and (3.33) , the singular boundary integral equation (3.29) can be evaluated by the linear system

$$P(\theta_j) + \sum_{k=0}^{2n-1} P(\theta_k)\{-R_j^n(\theta_k) + \frac{1}{2n}[Q(\theta_j,\theta_k) - N(\theta_j,\theta_k)]\}$$
$$= \sum_{k=0}^{2n-1}[-R_j^n(\theta_k) + \frac{1}{2n}Q(\theta_j,\theta_k)]\left\{\kappa(\theta_k) + \mu[1 - \frac{\widetilde{\sigma}}{2d}(r^2(\theta_k) + \frac{2r^2(\theta_k)}{\sqrt{r^2(\theta_k)+(r'(\theta_k))^2}})]\right\},$$
$$j = 0,1,2,...,2n-1, \quad (3.35)$$

with the quadrature weights

$$R_j^n(\theta_k) = -\frac{1}{n}\{\sum_{m=1}^{n-1}\frac{1}{m}cosm(\theta_k-\theta_j) + \frac{1}{2n}cosn(\theta_k-\theta_j)\}, \quad j = 0,1,2,...,2n-1, \quad (3.36)$$

and

$$\kappa(\theta) = \frac{r^2(\theta)+2(r'(\theta))^2 - r(\theta)r''(\theta)}{(r^2(\theta)+(r'(\theta))^2)^{\frac{3}{2}}}. \quad (3.37)$$

We wish to point out that once the values of $P(\theta_0), P(\theta_1), ..., P(\theta_{2n-1})$ are determined by (3.35) , we can also use (3.35) to define the values $P(\overline{\theta})$ for all $\overline{\theta}$ [17]

$$P(\overline{\theta}) := \sum_{k=0}^{2n-1} P(\theta_k)\{R^n(\theta_k) - \frac{1}{2n}[Q(\overline{\theta},\theta_k) - N(\overline{\theta},\theta_k)]\}$$
$$+ \sum_{k=0}^{2n-1}[-R^n(\theta_k) + \frac{1}{2n}Q(\overline{\theta},\theta_k)]\left\{\kappa(\theta_k) + \mu[1 - \frac{\widetilde{\sigma}}{2d}(r^2(\theta_k) + \frac{2r^2(\theta_k)}{\sqrt{r^2(\theta_k)+(r'(\theta_k))^2}})]\right\}, \quad (3.38)$$

with

$$R^n(\theta_k) = -\frac{1}{n}\{\sum_{m=1}^{n-1}\frac{1}{m}cosm(\theta_k-\overline{\theta}) + \frac{1}{2n}cosn(\theta_k-\overline{\theta})\}. \quad (3.39)$$

4. Method of Characteristics

We consider the boundary velocity equation

$$\frac{\partial r(\theta,t)}{\partial t} = v_r = v_n \cdot \frac{\sqrt{r^2(\theta,t) + (r_\theta(\theta,t))^2}}{r(\theta,t)}. \tag{4.1}$$

It follows from (4.1)

$$\begin{aligned} & F(\theta,t,r,r_\theta,r_t,r_{\theta\theta}) = \frac{\partial r(\theta,t)}{\partial t} - v_n \cdot \frac{\sqrt{r^2(\theta,t) + r_\theta^2(\theta,t)}}{r(\theta,t)} \\ = \;& r_t - (p(\theta,t) - \frac{r^2(\theta,t) + 2r_\theta^2(\theta,t) - r(\theta,t)r_{\theta\theta}(\theta,t)}{(r^2(\theta,t) + r_\theta^2(\theta,t))^{\frac{3}{2}}}) \cdot \frac{\sqrt{r^2(\theta,t) + r_\theta^2(\theta,t)}}{r(\theta,t)} \\ \stackrel{\Delta}{=} \;& r_t - (\psi(\theta,t) - H(r,r_\theta,r_{\theta\theta}))W(r,r_\theta) = 0, \end{aligned} \tag{4.2}$$

where $v_n = -\frac{\partial p(\mathbf{x},t)}{\partial n} = p(\mathbf{x},t) - \kappa = p(\theta,t) - \frac{r^2(\theta,t)+2r_\theta^2(\theta,t)-r(\theta,t)r_{\theta\theta}(\theta,t)}{(r^2(\theta,t)+r_\theta^2(\theta,t))^{\frac{3}{2}}}$, $\psi(\theta,t) \stackrel{\Delta}{=} p(\theta,t)$, $H(r,r_\theta,r_{\theta\theta}) \stackrel{\Delta}{=} \frac{r^2(\theta,t)+2r_\theta^2(\theta,t)-r(\theta,t)r_{\theta\theta}(\theta,t)}{(r^2(\theta,t)+r_\theta^2(\theta,t))^{\frac{3}{2}}}$ and $W(r,r_\theta) \stackrel{\Delta}{=} \frac{\sqrt{r^2(\theta,t)+r_\theta^2(\theta,t)}}{r(\theta,t)}$.

The characteristic equations of nonlinear PDE (4.2) are given by the following ODEs

$$\begin{aligned} \frac{d\theta}{ds} &= H_{r_\theta}(r,r_\theta,r_{\theta\theta})W(r,r_\theta) - (\psi(\theta,t) - H(r,r_\theta,r_{\theta\theta}))W_{r_\theta}(r,r_\theta), \quad \frac{dt}{ds} = 1, \\ \frac{dr_\theta}{ds} &= \psi_\theta(\theta,t)W(r,r_\theta) - [H_r(r,r_\theta,r_{\theta\theta})W(r,r_\theta) - (\psi(\theta,t) - H(r,r_\theta,r_{\theta\theta}))W_r(r,r_\theta)]r_\theta, \\ \frac{dr_t}{ds} &= \psi_t(\theta,t) - [H_r(r,r_\theta,r_{\theta\theta})W(r,r_\theta) - (\psi(\theta,t) - H(r,r_\theta,r_{\theta\theta}))W_r(r,r_\theta)]r_t \\ \frac{dr_{\theta\theta}}{ds} &= \Big[\psi_{\theta\theta} - [H_{rr}r_\theta + H_{rr_\theta}r_{\theta\theta}]r_\theta + H_r r_{\theta\theta} + [H_{r_\theta r}r_\theta + H_{r_\theta r_\theta}r_{\theta\theta}]r_{\theta\theta}\Big]W \\ &\quad +2[\psi_\theta - H_r r_\theta - H_{r_\theta}r_{\theta\theta}](W_r r_\theta + W_{r_\theta}r_{\theta\theta}) + (\psi - H) \\ &\quad \Big[(W_{rr}r_\theta + W_{rr_\theta}r_{\theta\theta})r_\theta + W_r r_{\theta\theta} + (W_{r_\theta r}r_\theta + W_{r_\theta r_\theta}r_{\theta\theta})r_{\theta\theta}\Big], \\ \frac{dr}{ds} &= [H_{r_\theta}(r,r_\theta,r_{\theta\theta})W(r,r_\theta) - (\psi(\theta,t) - H(r,r_\theta,r_{\theta\theta}))W_{r_\theta}(r,r_\theta)]r_\theta + r_t. \end{aligned} \tag{4.3}$$

Note that the derivatives of r_t are calculated by

$$r_{\theta t} = [\psi_\theta - H_r r_\theta - H_{r_\theta}r_{\theta\theta} - H_{r_{\theta\theta}}r_{\theta\theta\theta}]W + (\psi - H)(W_r r_\theta + W_{r_\theta}r_{\theta\theta}), \tag{4.4}$$

and

$$\begin{aligned} r_{\theta\theta t} &= \Big[\psi_{\theta\theta} - [H_{rr}r_\theta + H_{rr_\theta}r_{\theta\theta} + H_{rr_{\theta\theta}}r_{\theta\theta\theta}]r_\theta + H_r r_{\theta\theta} + [H_{r_\theta r}r_\theta + H_{r_\theta r_\theta}r_{\theta\theta} + H_{r_\theta r_{\theta\theta}}r_{\theta\theta\theta}]r_{\theta\theta} \\ &\quad + H_{r_\theta}r_{\theta\theta\theta} + [H_{r_{\theta\theta}r}r_\theta + H_{r_{\theta\theta}r_\theta}r_{\theta\theta} + H_{r_{\theta\theta}r_{\theta\theta}}r_{\theta\theta\theta}]r_{\theta\theta\theta} + H_{r_{\theta\theta}}r_{\theta\theta\theta\theta}\Big]W \\ &\quad + 2[\psi_\theta - H_r r_\theta - H_{r_\theta}r_{\theta\theta} - H_{r_{\theta\theta}}r_{\theta\theta\theta}](W_r r_\theta + W_{r_\theta}r_{\theta\theta}) + (\psi - H) \\ &\quad \Big[(W_{rr}r_\theta + W_{rr_\theta}r_{\theta\theta})r_\theta + W_r r_{\theta\theta} + (W_{r_\theta r}r_\theta + W_{r_\theta r_\theta}r_{\theta\theta})r_{\theta\theta} + W_{r_\theta}r_{\theta\theta\theta}\Big]. \end{aligned} \tag{4.5}$$

We decompose the time interval $[0, T]$ with grid points $t_m = m\Delta t$ for $m = 0, 1, 2..., M$, where $\Delta t = \frac{T}{M}$ and M is a positive integer.

From (4.3), it is easy to get the following iterative formulas to compute numerically the free boundary at time T.

$$\begin{aligned} \frac{\theta^{m+1} - \theta^m}{\Delta t} &= H^m_{r_\theta}(r^m, r^m_\theta, r^m_{\theta\theta})W^m(r^m, r^m_\theta) - (\psi^m(\theta^m, m\Delta t) - H^m(r^m, r^m_\theta, r^m_{\theta\theta})) \\ &\quad W^m_{r_\theta}(r^m, r^m_\theta), \\ \frac{r^{m+1}_\theta(\theta^{m+1}) - r^m_\theta(\theta^m)}{\Delta t} &= \psi^m_\theta(\theta^m, m\Delta t)W^m(r^m, r^m_\theta) - [H^m_r(r^m, r^m_\theta, r^m_{\theta\theta})W^m(r^m, r^m_\theta) \\ &\quad -(\psi^m(\theta^m, m\Delta t) - H^m(r^m, r^m_\theta, r^m_{\theta\theta}))W^m_r(r^m, r^m_\theta)]r^m_\theta, \\ \frac{r^{m+1}_t(\theta^{m+1}) - r^m_t(\theta^m)}{\Delta t} &= \psi^m_t(\theta^m, m\Delta t) - [H^m_r(r^m, r^m_\theta, r^m_{\theta\theta})W^m(r^m, r^m_\theta) - (\psi^m(\theta^m, m\Delta t) \\ &\quad -H^m(r^m, r^m_\theta, r^m_{\theta\theta}))W^m_r(r^m, r^m_\theta)]r^m_t, \\ \frac{r^{m+1}_{\theta\theta}(\theta^{m+1}) - r^m_{\theta\theta}(\theta^m)}{\Delta t} &= \Big[\psi^m_{\theta\theta} - [H^m_{rr}r^m_\theta + H^m_{rr_\theta}r^m_{\theta\theta}]r^m_\theta + H^m_r r^m_{\theta\theta} + [H^m_{r_\theta r}r^m_\theta + H^m_{r_\theta r_\theta}r^m_{\theta\theta}]r^m_{\theta\theta}\Big]W^m \\ &\quad +2[\psi^m_\theta - H^m_r r^m_\theta - H^m_{r_\theta}r^m_{\theta\theta}](W^m_r r^m_\theta + W^m_{r_\theta}r^m_{\theta\theta}) + (\psi^m - H^m) \\ &\quad \Big[(W^m_{rr}r^m_\theta + W^m_{rr_\theta}r^m_{\theta\theta})r^m_\theta + W^m_r r^m_{\theta\theta} + (W^m_{r_\theta r}r_\theta + W^m_{r_\theta r_\theta}r^m_{\theta\theta})r^m_{\theta\theta}\Big], \\ \frac{r^{m+1}(\theta^{m+1}) - r^m(\theta^m)}{\Delta t} &= [H^m_{r_\theta}(r^m, r^m_\theta, r^m_{\theta\theta})W^m(r^m, r^m_\theta) - (\psi^m(\theta^m, m\Delta t) - H^m(r^m, r^m_\theta, r^m_{\theta\theta})) \\ &\quad W^m_{r_\theta}(r^m, r^m_\theta)]r^m_\theta + r^m_t, \end{aligned} \tag{4.6}$$

with

$$(\theta^0, r^0(\theta^0), r^0_\theta(\theta^0), r^0_t(\theta^0), r^0_{\theta\theta}(\theta^0)) = (\theta, r_0(\theta), \frac{\partial r_0(\theta, 0)}{\partial\theta}, \frac{\partial r_0(\theta, 0)}{\partial t}, \frac{\partial^2 r_0(\theta, 0)}{\partial\theta^2}), \tag{4.7}$$

and $r_t^0 = (\psi^0(\theta, 0) - H(r^0, r_\theta^0, r_{\theta\theta}^0))W(r^0, r_\theta^0)$.

Note that the superscript m denotes the numerical solutions at $t = m\Delta t$ time level.

In above formulation, the mesh size of θ is not a fixed quantity but changes along the characteristic curve in time.

5. Numerical Integral Formula with Weakly Singular Kernel

In this section, we deduce the numerical integral formula (3.23) with weakly singular kernel and provide the convergence and error for such approximation schemes.

We have used the following two numerical integrations in section 3.

(1) A weakly singular operator with a logarithmic singularity

$$(A\psi)(\overline{\theta}) = \frac{1}{2\pi}\int_0^{2\pi} ln(4sin^2\frac{\overline{\theta}-\theta}{2})\psi(\theta)d\theta, \qquad \overline{\theta} \in [0, 2\pi], \tag{5.1}$$

is approximated by a numerical integration operator

$$(A_n\psi)(\overline{\theta}) = \sum_{j=0}^{2n-1} R_j^n(\overline{\theta})\psi(\theta_j), \qquad \overline{\theta} \in [0, 2\pi], \tag{5.2}$$

with the quadrature weights

$$R_j^n(\overline{\theta}) = -\frac{1}{n}\{\sum_{m=1}^{n-1}\frac{1}{m}cosm(\overline{\theta}-\theta_j) + \frac{1}{2n}cosn(\overline{\theta}-\theta_j)\}, \quad j = 0, 1, 2, ..., 2n-1. \tag{5.3}$$

(2) A integral operator with analytic and 2π-periodic kernel

$$(B\psi)(\overline{\theta}) = \frac{1}{2\pi}\int_0^{2\pi} M(\theta, \overline{\theta})\psi(\theta)d\theta, \tag{5.4}$$

is approximated by composite trapezoidal rule

$$(B_n\psi)(\overline{\theta}) = \frac{1}{2n}\sum_{j=0}^{2n-1} M(\frac{j\pi}{n}, \overline{\theta})\psi(\frac{j\pi}{n}). \tag{5.5}$$

We now deduce the numerical approximates (5.2) of the integral (5.1).

The interpolation of $\psi(\theta)$ in (5.1) is given by

$$P_{2n}\psi(\theta) = \sum_{j=0}^{2n-1} L_j(\theta)\psi(\theta_j), \tag{5.6}$$

with $P_{2n}\psi(\theta_j) = \psi(\theta_j), \quad j = 0, 1, 2, ..., (2n-1)$.

Here $L_0(\theta), L_1(\theta), ..., L_{2n-1}(\theta)$ denote the Lagrange basises which have the interpolation property

$$L_k(\theta_j) = \delta_{jk}, \quad j, k = 0, 1, 2, ..., (2n-1), \tag{5.7}$$

and δ_{jk} is the Kronecker symbol with $\delta_{jk} = 1$ as $k = j$, $\delta_{jk} = 0$ as $k \neq j$.

Hence, we derive

$$\begin{aligned}
(A_n\psi)(\overline{\theta}) &= \frac{1}{2\pi}\int_0^{2\pi} ln(4sin^2\frac{\overline{\theta}-\theta}{2}) \sum_{j=0}^{2n-1} L_j(\theta)\psi(\theta_j)d\theta \\
&= \sum_{j=0}^{2n-1} \psi(\theta_j)\frac{1}{2\pi}\int_0^{2\pi} ln(4sin^2\frac{\overline{\theta}-\theta}{2})L_j(\theta)d\theta \\
&= \sum_{j=0}^{2n-1} R_j^n(\overline{\theta})\psi(\theta_j), \qquad \overline{\theta} \in [0, 2\pi],
\end{aligned} \tag{5.8}$$

where

$$R_j^n(\overline{\theta}) = \frac{1}{2\pi}\int_0^{2\pi} ln(4sin^2\frac{\overline{\theta}-\theta}{2})L_j(\theta)d\theta. \tag{5.9}$$

The Lagrange basis for the trigonometric interpolation has the form [17]

$$L_j(\theta) = \frac{1}{2n}\{1 + 2\sum_{m=1}^{n-1} cosm(\theta-\theta_j) + cosn(\theta-\theta_j)\}, \ j = 0, 1, 2, ..., 2n-1. \tag{5.10}$$

Therefore, we have

$$\begin{aligned}
&R_j^n(\overline{\theta}) = \frac{1}{2\pi}\int_0^{2\pi} ln(4sin^2\frac{\overline{\theta}-\theta}{2})L_j(\theta)d\theta \\
&= \frac{1}{2\pi}\int_0^{2\pi} ln(4sin^2\frac{\theta-\overline{\theta}}{2}) \cdot \frac{1}{2n}\{1 + 2\sum_{m=1}^{n-1} cosm(\theta-\theta_j) + cosn(\theta-\theta_j)\}d\theta
\end{aligned}$$

$$= \frac{1}{4n\pi}\int_0^{2\pi} ln(4sin^2\frac{\theta-\overline{\theta}}{2})\{1+2\sum_{m=1}^{n-1} cosm[(\theta-\overline{\theta})+(\overline{\theta}-\theta_j)]+cosn[(\theta-\overline{\theta})+(\overline{\theta}-\theta_j)]\}d\theta$$

$$= \frac{1}{4n\pi}\int_0^{2\pi} ln(4sin^2\frac{\theta-\overline{\theta}}{2})\{1+2\sum_{m=1}^{n-1}[cosm(\theta-\overline{\theta})cosm(\overline{\theta}-\theta_j)-sinm(\theta-\overline{\theta})sinm(\overline{\theta}-\theta_j)]$$
$$+cosn(\theta-\overline{\theta})cosn(\overline{\theta}-\theta_j)-sinn(\theta-\overline{\theta})sinn(\overline{\theta}-\theta_j)\}d\theta. \quad (5.11)$$

Using [17]

$$\frac{1}{2\pi}\int_0^{2\pi} ln(4sin^2\frac{\varphi}{2})e^{im\varphi}d\varphi = \begin{cases} 0 & m=0, \\ -\frac{1}{|m|} & m=\pm1,\pm2,..., \end{cases} \quad (5.12)$$

we obtain

$$R_j^n(\overline{\theta}) = -\frac{1}{n}\{\sum_{m=1}^{n-1}\frac{1}{m}cosm(\overline{\theta}-\theta_j)+\frac{1}{2n}cosn(\overline{\theta}-\theta_j)\}, j=0,1,2,...,2n-1. \quad (5.13)$$

Thus, we have completed the deduction of (5.1),(5.2) and (5.3), i.e., (3.23).

Moreover, the sequence A_n given by (5.2) is collectively compact and pointwise convergent to the integral operator A with the logarithmic singularity given by (5.1). And the quadrature error is exponentially decreasing provided ψ is analytic and 2π-periodic. (see[17])

Let the kernel M and ψ be analytic and 2π-periodic, then the error for the composite trapezoidal quadrature can be estimated by [17]

$$(B\psi)(\overline{\theta})-(B_n\psi)(\overline{\theta}) \le C(cothns-1) = C\frac{e^{2ns}+1}{e^{2ns}-1}$$
$$= C\frac{2}{e^{2ns}-1} \le C\frac{3}{e^{2ns}} = 3Ce^{-2ns}, \quad (take\ n \ge \frac{1}{2s}ln3), \quad (5.14)$$

where C and s depend on M and ψ. The error decays at least exponentially.

In addition, assume the error of the time level $m\Delta t$ is β, we consider the error of the time level $(m+1)\Delta t$

$$|r^{m+1}-r(t+\Delta t)| = |r^{m+1}-r(t)-r'(t)\Delta t-\frac{r''(t)}{2!}(\Delta t)^2-\ ...\ |$$
$$= |r^{m+1}-r^m+r^m-r(t)-r'(t)\Delta t-\frac{r''(t)}{2!}(\Delta t)^2-\ ...\ |$$

$$
\begin{aligned}
&\leq |r^{m+1}-r^m| + |r^m - r(t)| + |-r'(t)\Delta t - \frac{r''(t)}{2!}(\Delta t)^2 - \ ... \ | \\
&\leq |v_r^m \cdot \triangle t| + \beta + |r'(t)\Delta t + \frac{r''(t)}{2!}(\Delta t)^2 + \ ... \ | \\
&\approx |(\frac{\partial p}{\partial n})^m \cdot \frac{\sqrt{(r^m)^2 + ((r_\theta)^m)^2}}{r^m} \cdot \triangle t| + \beta + |r'(t)\Delta t + \frac{r''(t)}{2!}(\Delta t)^2 + \ ... \ |, \quad (5.15)
\end{aligned}
$$

where $\frac{\partial p}{\partial n} = \kappa - p$.

6. Numerical Experiments

Our numerical method is that at $m\Delta t$ time level, we solve approximate solution $\sigma_k^m (k = 0, 1, 2, ..., 2n-1)$ of $\sigma(k\Delta\theta, m\Delta t)(k = 0, 1, 2, ..., 2n-1)$ on the boundary Γ^m at $\theta = \theta_0^m, \theta_1^m, \theta_2^m, ...\theta_{2n-1}^m$ by the numerical scheme(3.26) of the boundary integral equation(2.6); Substituting $\sigma_k^m (k = 0, 1, 2, ..., 2n-1)$ into the numerical scheme (3.35)of boundary integral equation(2.7), we solve approximate solution $P_k^m (k = 0, 1, 2, ...2n-1)$ of $P(k\Delta\theta, m\Delta t)(k = 0, 1, 2, ...2n-1)$ on the boundary Γ^m at $\theta = \theta_0^m, \theta_1^m, \theta_2^m, ...\theta_{2n-1}^m$; Then, using (4.6), we can obtain the new nodes $\theta = \theta_0^{m+1}, \theta_1^{m+1}, \theta_2^{m+1}, ...\theta_{2n-1}^{m+1}$ and the new boundary $r_k^{(m+1)}$ $(k = 0, 1, 2, ..., 2n-1)$ at time level $(m+1)\Delta t$ according to the boundary r_k^m $(k = 0, 1, 2, ..., 2n-1)$ and $P_k^m (k = 0, 1, 2, ..., 2n-1)$. Afterwards, we simulate the boundary Γ^{m+1} of the tumor by piecewise quadratic curve at every node $\theta = \theta_0^{m+1}, \theta_1^{m+1}, \theta_2^{m+1}, ...\theta_{2n-1}^{m+1}$.

Similar method, at $(m+1)\Delta t$ time level, we solve $\sigma_k^{m+1} (k = 0, 1, 2, 3, ..., 2n-1)$ from (3.28) at $\theta = \theta_0^{m+1}, \theta_1^{m+1}, \theta_2^{m+1}, ...\theta_{2n-1}^{m+1}$ on the new boundary r_k^{m+1} $(k = 0, 1, 2, ..., 2n-1)$; Next, we compute $P_k^{m+1} (k = 0, 1, 2, ...2n-1)$ from (3.35) at $\theta = \theta_0^{m+1}, \theta_1^{m+1}, \theta_2^{m+1}, ...\theta_{2n-1}^{m+1}$ on the boundary Γ^{m+1} at $\theta = \theta_0^{m+1}, \theta_1^{m+1}, \theta_2^{m+1}, ...\theta_{2n-1}^{m+1}$ after substituting $\sigma_k^{m+1} (k = 0, 1, 2, ..., 2n-1)$ into (3.35); Then, using (4.6), ..., Eventually, we derive the free boundary at the final time T.

Furthermore, we construct the numerical example to test our numerical method.

We consider a perturbed boundary $\Gamma(t) : r = R(t) + \varepsilon f(\theta)$, where $R(t)$ is the radius of a evolving circle and ε is the dimensionless perturbation amplitude.

We now turn our attention to compute nonradially symmetric solutions of the form

$$
\sigma|_{r=R(t)+\varepsilon f(\theta)} = \sigma_s|_{r=R(t)+\varepsilon f(\theta)} + \varepsilon\sigma_\varepsilon|_{r=R(t)+\varepsilon f(\theta)} + O(\varepsilon^2), \quad (6.1)
$$

$$p|_{r=R(t)+\varepsilon f(\theta)} = p_s|_{r=R(t)+\varepsilon f(\theta)} + \varepsilon p_\varepsilon|_{r=R(t)+\varepsilon f(\theta)} + O(\varepsilon^2), \tag{6.2}$$

where σ_s and p_s are the radial symmetrical solutions.

From (6.1), we can deduce

$$\begin{aligned}
& \varepsilon(\sigma_\varepsilon + \frac{\partial \sigma_\varepsilon}{\partial n})|_{r=R(t)} = \varepsilon(\sigma_\varepsilon + \frac{\partial \sigma_\varepsilon}{\partial n})|_{r=R(t)+\varepsilon f(\theta)} + O(\varepsilon^2) \\
= \;& (\sigma + \frac{\partial \sigma}{\partial n})|_{r=R(t)+\varepsilon f(\theta)} - (\sigma_s + \frac{\partial \sigma_s}{\partial n})|_{r=R(t)+\varepsilon f(\theta)} + O(\varepsilon^2) \\
= \;& 1 - [(\sigma_s + \frac{\partial \sigma_s}{\partial n})|_{r=R(t)} + \varepsilon \frac{\partial(\sigma_s + \frac{\partial \sigma_s}{\partial n})}{\partial r}(R(t))f(\theta) + O(\varepsilon^2)] \\
= \;& -\varepsilon \frac{\partial}{\partial r}(\sigma_s + \frac{\partial \sigma_s}{\partial n})(R(t))f(\theta) + O(\varepsilon^2).
\end{aligned} \tag{6.3}$$

In the following calculation, we neglect the higher order terms

$$\left\{ \begin{array}{rcll} -\Delta \sigma_\varepsilon & + & \sigma_\varepsilon = 0 & \text{in } B_{R(t)}, \\ \sigma_\varepsilon + \frac{\partial \sigma_\varepsilon}{\partial r} & = & -\frac{\partial}{\partial r}(\sigma_s + \frac{\partial \sigma_s}{\partial r})(R(t))f(\theta) & \text{on } \partial B_{R(t)}, \end{array} \right. \tag{6.4}$$

where the boundary $\partial B_{R(t)} : r = R(t)$.

The solution for the problem (6.4) is given as follows

$$\sigma_\varepsilon(r,t) = -\frac{I_0(r)}{I_0(R(t)) + I_1(R(t))} \frac{\partial}{\partial r}(\sigma_s + \frac{\partial \sigma_s}{\partial r})(R(t))f(\theta). \tag{6.5}$$

In addition, we have the mean curvature of the boundary

$$\kappa = \frac{1}{R(t)} - \frac{\varepsilon}{R^2(t)}[f(\theta) + f^{"}(\theta)] + O(\varepsilon^2). \tag{6.6}$$

To compute p_ε, we employ the same computational strategy as used in (6.3)

$$\begin{aligned}
& \varepsilon(p_\varepsilon + \frac{\partial p_\varepsilon}{\partial n})|_{r=R(t)} = \varepsilon(p_\varepsilon + \frac{\partial p_\varepsilon}{\partial n})|_{r=R(t)+\varepsilon f(\theta)} + O(\varepsilon^2) \\
= \;& (p + \frac{\partial p}{\partial n})|_{r=R(t)+\varepsilon f(\theta)} - (p_s + \frac{\partial p_s}{\partial n})|_{r=R(t)+\varepsilon f(\theta)} + O(\varepsilon^2) \\
= \;& \kappa - [(p_s + \frac{\partial p_s}{\partial r})|_{r=R(t)} + \varepsilon \frac{\partial(p_s + \frac{\partial p_s}{\partial r})}{\partial r}(R(t))f(\theta) + O(\varepsilon^2)]
\end{aligned}$$

$$
\begin{aligned}
&= \kappa - \frac{1}{R(t)} - \varepsilon\frac{\partial}{\partial r}(p_s + \frac{\partial p_s}{\partial r})(R(t))f(\theta) + O(\varepsilon^2) \\
&= [\frac{1}{R(t)} - \frac{\varepsilon}{R^2(t)}[f(\theta) + f^{"}(\theta)] + O(\varepsilon^2)] - \frac{1}{R(t)} - \varepsilon\frac{\partial}{\partial r}(p_s + \frac{\partial p_s}{\partial r})(R(t))f(\theta) + O(\varepsilon^2) \\
&= -\frac{\varepsilon}{R^2(t)}[f(\theta) + f^{"}(\theta)] - \varepsilon\frac{\partial}{\partial r}(p_s + \frac{\partial p_s}{\partial r})(R(t))f(\theta) + O(\varepsilon^2).
\end{aligned}
$$

Dropping the higher terms, we get

$$
\left\{
\begin{array}{rcll}
-\Delta p_\varepsilon &=& \mu\sigma_\varepsilon, & \text{in } B_{R(t)}, \\
\sigma_\varepsilon + \frac{\partial\sigma_\varepsilon}{\partial r} &=& -\frac{\partial}{\partial r}(\sigma_s + \frac{\partial\sigma_s}{\partial r})(R(t))f(\theta), & \text{on } \partial B_{R(t)}, \\
p_\varepsilon + \frac{\partial p_\varepsilon}{\partial r} &=& -\frac{\partial}{\partial r}(p_s + \frac{\partial p_s}{\partial r})(R(t))f(\theta) - \frac{1}{R^2(t)}[f(\theta) + f^{"}(\theta)], & \text{on } \partial B_{R(t)}.
\end{array}
\right.
$$

i.e.,

$$
\left\{
\begin{array}{rcll}
-\Delta(p_\varepsilon + \mu\sigma_\varepsilon) &=& 0, & \text{in } B_{R(t)}, \\
p_\varepsilon + \mu\sigma_\varepsilon + \frac{\partial}{\partial r}(p_\varepsilon + \mu\sigma_\varepsilon) &=& -\frac{\partial}{\partial r}(p_s + \frac{\partial p_s}{\partial r})(R(t))f(\theta) - \frac{1}{R^2(t)}[f(\theta) + f^{"}(\theta)] & \\
& & -\mu\frac{\partial}{\partial r}(\sigma_s + \frac{\partial\sigma_s}{\partial r})(R(t))f(\theta). & \text{on } \partial B_{R(t)}.
\end{array}
\right. \tag{6.7}
$$

For simplicity's sake, we take $f(\theta) = cosl\theta,\ l = 2, 3, 4, ...$, so

$$
\begin{aligned}
&-\frac{\partial}{\partial r}(p_s + \frac{\partial p_s}{\partial r})(R(t))f(\theta) - \frac{1}{R^2(t)}[f(\theta) + f^{"}(\theta)] - \mu\frac{\partial}{\partial r}(\sigma_s + \frac{\partial\sigma_s}{\partial r})(R(t))f(\theta) \\
&= [-\frac{\partial}{\partial r}(p_s + \frac{\partial p_s}{\partial r})(R(t)) - \frac{1}{R^2(t)} - \mu\frac{\partial}{\partial r}(\sigma_s + \frac{\partial\sigma_s}{\partial r})(R(t)) + \frac{l^2}{R^2(t)}]cosl\theta. \quad (6.8)
\end{aligned}
$$

We are now in a position to solve the problem (6.7).
It is known that the general solution of Laplace equation has the form

$$
p_\varepsilon + \mu\sigma_\varepsilon = a_0 + \sum_{n=1}^{\infty}[a_n r^n cosn\theta + b_n r^n sinn\theta], \tag{6.9}
$$

which yields

$$
p_\varepsilon + \mu\sigma_\varepsilon + \frac{\partial}{\partial r}(p_\varepsilon + \mu\sigma_\varepsilon) = a_0 + \sum_{n=1}^{\infty}[a_n(r^n + nr^{n-1})cosn\theta + b_n(r^n + nr^{n-1})sinn\theta]. \tag{6.10}
$$

It follows from the boundary condition of problem (6.7) that

$$
[-\frac{\partial}{\partial r}(p_s + \frac{\partial p_s}{\partial r})(R(t)) - \frac{1}{R^2(t)} - \mu\frac{\partial}{\partial r}(\sigma_s + \frac{\partial\sigma_s}{\partial r})(R(t)) + \frac{l^2}{R^2(t)}]cosl\theta
$$

$$= a_0 + \sum_{n=1}^{\infty}[a_n(R^n(t) + nR^{n-1}(t))cosn\theta + b_n(R^n(t) + nR^{n-1}(t))sinn\theta]. \quad (6.11)$$

It is easy to calculate from (6.11)

$$\begin{aligned}
&[-\frac{\partial}{\partial r}(p_s + \frac{\partial p_s}{\partial r})(R(t)) - \frac{1}{R^2(t)} - \mu\frac{\partial}{\partial r}(\sigma_s + \frac{\partial \sigma_s}{\partial r})(R(t)) + \frac{l^2}{R^2(t)}] \int_0^{2\pi} cos^2 l\theta d\theta \\
= \; & a_0 \int_0^{2\pi} cosl\theta d\theta + \sum_{n=1}^{\infty}[a_n(R^n(t) + nR^{n-1}(t)) \int_0^{2\pi} cosl\theta cosn\theta d\theta \\
& + b_n(R^n(t) + nR^{n-1}(t)) \int_0^{2\pi} cosl\theta sinn\theta d\theta] \\
= \; & a_l(R^l(t) + lR^{l-1}(t)) \int_0^{2\pi} cos^2 l\theta d\theta.
\end{aligned}$$

Thus

$$a_l = \frac{1}{R^l(t) + lR^{l-1}(t)}[-\frac{\partial}{\partial r}(p_s + \frac{\partial p_s}{\partial r})(R(t)) - \frac{1}{R^2(t)} - \mu\frac{\partial}{\partial r}(\sigma_s + \frac{\partial \sigma_s}{\partial r})(R(t)) + \frac{l^2}{R^2(t)}].$$

We can also determine that $a_n = 0, n \neq l$ and $b_n = 0, n = 1, 2, ...$
Therefore, we yield the solution of problem(6.7)

$$p_\varepsilon + \mu\sigma_\varepsilon = \frac{r^l}{R^l(t) + lR^{l-1}(t)}[-\frac{\partial}{\partial r}(p_s + \frac{\partial p_s}{\partial r})(R(t)) - \frac{1}{R^2(t)} - \mu\frac{\partial}{\partial r}(\sigma_s + \frac{\partial \sigma_s}{\partial r})(R(t)) + \frac{l^2}{R^2(t)}]cosl\theta,$$

which implies

$$p_\varepsilon = -\mu\sigma_\varepsilon - \frac{r^l}{R^l(t) + lR^{l-1}(t)}[\frac{\partial}{\partial r}(p_s + \frac{\partial p_s}{\partial r})(R(t)) + \frac{1}{R^2(t)} + \mu\frac{\partial}{\partial r}(\sigma_s + \frac{\partial \sigma_s}{\partial r})(R(t)) - \frac{l^2}{R^2(t)}]cosl\theta, \quad (6.12)$$

and

$$\begin{aligned}
\frac{\partial p_\varepsilon(R(t))}{\partial r} = \; & -\mu\frac{\partial \sigma_\varepsilon}{\partial r}(R(t)) - \frac{l}{R(t) + l}[\frac{\partial}{\partial r}(p_s + \frac{\partial p_s}{\partial r})(R(t)) + \frac{1}{R^2(t)} + \mu\frac{\partial}{\partial r}(\sigma_s + \frac{\partial \sigma_s}{\partial r})(R(t)) \\
& - \frac{l^2}{R^2(t)}]cosl\theta. \quad (6.13)
\end{aligned}$$

As a result, we obtain

$$p|_{r=R(t)+\varepsilon f(\theta)} = p|_{r=R(t)} + \varepsilon p'|_{r=R(t)} f(\theta) + O(\varepsilon^2)$$

$$= (p_s + \varepsilon p_\varepsilon + O(\varepsilon^2))|_{r=R(t)} + \varepsilon(p_s + \varepsilon p_\varepsilon + O(\varepsilon^2))'|_{r=R(t)} f(\theta) + O(\varepsilon^2)$$
$$= p_s(R(t)) + \varepsilon[p_\varepsilon(R(t)) + \frac{\partial p_s}{\partial r}(R(t))f(\theta)] + O(\varepsilon^2), \tag{6.14}$$

and

$$\begin{aligned} & \frac{\partial p}{\partial n}|_{r=R(t)+\varepsilon f(\theta)} = \frac{\partial p}{\partial n}|_{r=R(t)} + \varepsilon(\frac{\partial p}{\partial n})'|_{r=R(t)} f(\theta) + O(\varepsilon^2) \\ = & \frac{\partial[p_s + \varepsilon p_\varepsilon + O(\varepsilon^2)]}{\partial r}|_{r=R(t)} + \varepsilon\frac{\partial}{\partial r}(\frac{\partial[p_s + \varepsilon p_\varepsilon + O(\varepsilon^2)]}{\partial r})|_{r=R(t)} f(\theta) + O(\varepsilon^2) \\ = & \frac{\partial p_s(R(t))}{\partial r}) + \varepsilon[\frac{\partial^2 p_s(R(t))}{\partial r^2} f(\theta) + \frac{\partial p_\varepsilon(R(t))}{\partial r}] + O(\varepsilon^2) = -v_n. \end{aligned} \tag{6.15}$$

Furthermore, we calculate the radially symmetric solutions $p_s(R(t))$, $\frac{\partial p_s(R(t))}{\partial r}$ and $\frac{\partial^2 p_s(R(t))}{\partial r^2}$ in above formula (6.14) and (6.15).

We consider the following boundary problem

$$\begin{cases} -\Delta\sigma + \sigma = 0 & \text{in } B_{R(t)}, \\ -\Delta p = \mu(\sigma - \widetilde{\sigma}) & \text{in } B_{R(t)}, \\ \sigma + \frac{\partial\sigma}{\partial n} = 1 & \text{on } \partial B_{R(t)}, \\ p + \frac{\partial p}{\partial n} = \kappa & \text{on } \partial B_{R(t)}, \\ \frac{\partial p}{\partial n} = -v_n & \text{on } \partial B_{R(t)}. \end{cases} \tag{6.16}$$

Assume radial symmetrical solution $\sigma = \sigma_s(r,t)$ of

$$\begin{cases} -\Delta\sigma_s + \sigma_s = 0 & \text{in } B_{R(t)}, \\ \sigma_s + \frac{\partial\sigma_s}{\partial n} = 1 & \text{on } \partial B_{R(t)}, \end{cases} \tag{6.17}$$

we have

$$\begin{cases} \sigma_{srr} + \frac{1}{r}\sigma_{sr} - \sigma_s = 0 & \text{in } B_{R(t)}, \\ \sigma_s + \frac{\partial\sigma_s}{\partial r} = 1 & \text{on } \partial B_{R(t)}. \end{cases}$$

Substituting the radial symmetrical solution $\sigma_s(\mathbf{x},t) = cI_0(r)$ of equation $\sigma_{srr} + \frac{1}{r}\sigma_{sr} - \sigma_s = 0$ into the boundary condition $\sigma_s + \frac{\partial\sigma_s}{\partial r} = 1$, we get

$$[cI_0(r) + cI_1(r)]|_{r=R(t)} = 1,$$

i.e.,

$$c = \frac{1}{I_0(R(t)) + I_1(R(t))}.$$

Therefore, the radial symmetrical solution of problem (6.17) is

$$\sigma_s(r,t) = \frac{I_0(r)}{I_0(R(t)) + I_1(R(t))}, \tag{6.18}$$

which yields that

$$\frac{\partial \sigma_s}{\partial n}(R(t)) = \frac{\partial \sigma_s}{\partial r}(R(t)) = \frac{I_0'(R(t))}{I_0(R(t)) + I_1(R(t))} = \frac{I_1(R(t))}{I_0(R(t)) + I_1(R(t))}, \tag{6.19}$$

and

$$\frac{\partial^2 \sigma_s(R(t))}{\partial r^2} = \frac{I_0''(R(t))}{I_0(R(t)) + I_1(R(t))} = \frac{I'_1(R(t))}{I_0(R(t)) + I_1(R(t))}, \tag{6.20}$$

where $I_0(r)$, $I_1(r)$ are the modified Bessel functions, $I_0(r) = \sum_{n=0}^{\infty} \frac{1}{(n!)^2}(\frac{r}{2})^{2n}$, $I_1(r) = \sum_{n=0}^{\infty} \frac{1}{n!(n+1)!}(\frac{r}{2})^{2n+1}$, $I_0'(r) = I_1(r)$.

Likewise, we consider the radial symmetrical solution of the following boundary problem

$$\begin{cases} \Delta(p_s + \mu\sigma_s) = \mu\widetilde{\sigma} & \text{in } B_{R(t)}, \\ \sigma_s + \frac{\partial \sigma_s}{\partial r} = 1 & \text{on } \partial B_{R(t)}, \\ p_s + \frac{\partial p_s}{\partial r} = \kappa & \text{on } \partial B_{R(t)}. \end{cases} \tag{6.21}$$

i.e.,

$$\begin{cases} (p_s + \mu\sigma_s)_{rr} + \frac{1}{r}(p_s + \mu\sigma_s)_r = \mu\widetilde{\sigma} & \text{in } B_{R(t)}, \\ (p_s + \mu\sigma_s) + \frac{\partial}{\partial r}(p_s + \mu\sigma_s) = \frac{1}{R(t)} + \mu & \text{on } \partial B_{R(t)}. \end{cases}$$

Substituting the radial symmetrical solution $p_s + \mu\sigma_s = \frac{\mu\widetilde{\sigma}}{4}r^2 + c$ of the equation $(p_s + \mu\sigma_s)_{rr} + \frac{1}{r}(p_s + \mu\sigma_s)_r = \mu\widetilde{\sigma}$ into the boundary condition $(p_s + \mu\sigma_s) + \frac{\partial}{\partial r}(p_s + \mu\sigma_s) = \frac{1}{R(t)} + \mu$, we obtain

$$[\frac{\mu\widetilde{\sigma}}{4}r^2 + c + \frac{\mu\widetilde{\sigma}}{2}r]|_{r=R(t)} = \frac{1}{R(t)} + \mu,$$

i.e.,

$$c = -\frac{\mu\widetilde{\sigma}}{4}R^2(t) - \frac{\mu\widetilde{\sigma}}{2}R(t) + \frac{1}{R(t)} + \mu.$$

Hence, the radial symmetrical solution of the problem (6.21) is

$$p_s + \mu\sigma_s = \frac{\mu\widetilde{\sigma}}{4}r^2 - \frac{\mu\widetilde{\sigma}}{4}R^2(t) - \frac{\mu\widetilde{\sigma}}{2}R(t) + \frac{1}{R(t)} + \mu,$$

i.e.,

$$p_s(r,t) = -\mu\sigma_s(r,t) + \frac{\mu\widetilde{\sigma}}{4}r^2 - \frac{\mu\widetilde{\sigma}}{4}R^2(t) - \frac{\mu\widetilde{\sigma}}{2}R(t) + \frac{1}{R(t)} + \mu, \quad (6.22)$$

which implies that

$$\frac{\partial p_s}{\partial n}(R(t)) = \frac{\partial p_s}{\partial r}(R(t)) = -\mu[\frac{\partial \sigma_s}{\partial r}(R(t)) - \frac{\widetilde{\sigma}}{2}R(t)] = -\mu[\frac{I_1(R(t))}{I_0(R(t)) + I_1(R(t))} - \frac{\widetilde{\sigma}}{2}R(t)], \quad (6.23)$$

and

$$\frac{\partial^2 p_s(R(t))}{\partial r^2} = -\mu[\frac{\partial^2 \sigma_s(R(t))}{\partial r^2} - \frac{\widetilde{\sigma}}{2}] = -\mu[\frac{I'_1(R(t))}{I_0(R(t)) + I_1(R(t))} - \frac{\widetilde{\sigma}}{2}]. \quad (6.24)$$

Now, we derive the numerical example as follows

Example I: On a perturbed boundary $\Gamma(t) : r = R(t) + \varepsilon cosl\theta$, $l = 2, 3, 4, ...,$ the analytical solutions of the problem (2.2) are given as follows:

$$\sigma|_{r=R(t)+\varepsilon cosl\theta} = \sigma_s(R(t)) + \varepsilon[\sigma_\varepsilon(R(t)) + \frac{\partial \sigma_s}{\partial r}(R(t))cosl\theta] + O(\varepsilon^2), \quad (6.25)$$

$$p|_{r=R(t)+\varepsilon cosl\theta} = p_s(R(t)) + \varepsilon[p_\varepsilon(R(t)) + \frac{\partial p_s}{\partial r}(R(t))cosl\theta] + O(\varepsilon^2), \quad (6.26)$$

and

$$\begin{aligned}\frac{\partial p}{\partial n}|_{r=R(t)+\varepsilon cosl\theta} &= -\mu[\frac{I_1(R(t))}{I_0(R(t)) + I_1(R(t))} - \frac{\widetilde{\sigma}}{2}R(t)] - \varepsilon\mu[\frac{I'_1(R(t))}{I_0(R(t)) + I_1(R(t))} - \frac{\widetilde{\sigma}}{2}]cosl\theta \\ &\quad -\varepsilon\mu\frac{\partial \sigma_\varepsilon}{\partial r}(R(t)) - \frac{\varepsilon l}{R(t) + l}[\frac{\partial}{\partial r}(p_s + \frac{\partial p_s}{\partial r})(R(t)) + \frac{1}{R^2(t)} \\ &\quad +\mu\frac{\partial}{\partial r}(\sigma_s + \frac{\partial \sigma_s}{\partial r})(R(t)) - \frac{l^2}{R^2(t)}]cosl\theta + O(\varepsilon^2) = -v_n. \end{aligned} \quad (6.27)$$

Next, we implement the numerical example above.

We take ε to be a small value 10^{-3} and the number of grid points $2n = 160$ on the boundary. Setting $\mu = 1.2$, $\widetilde{\sigma} = 0.6$. Our boundary smoothing technique is: At time step $t_m = m\Delta t(m = 0, 1, 2, ..., M)$, for each node $\theta_m^k(k = 0, 1, 2, ..., 2n-1)$, we fit a small quadratic curve r_k^m at each node by this node and its two adjacent nodes in $\left[\theta_{k-1}^m, \theta_{k+1}^m\right]$ $(k = 0, 1, 2, ..., 2n-1)$, and

totally fit $2n$ small quadratic curves $r_k^m (k = 0, 1, 2, ..., 2n-1)$ at $2n$ nodes so that there always is a local quadratic curve smoothly passing through each node, which can keep the local smoothness (the existence of until infinity derivatives at each node) of the boundary curve. In our numerical computation (3.35) (see (3.31), (3.32), (3.34), (3.37)), we use the values (3.4) of the piecewise quadratic curve and its until the second derivative at each node to compute $N(\theta_j, \theta_k), Q(\theta_j, \theta_k)$ and curvature $\kappa(\theta_k)$. As expected, the errors of our numerical experiments are $O(\varepsilon^2)$, where the errors measured are the difference between our nonlinear computation and the "analytical solution". In fact, the "analytical solution" is just the linear solution (the linear part of (6.25),(6.26) and (6.27)) in our numerical errors.

To test the convergence in time, using a very small Δt, we take the solution as the reference solution. Then using large time steps such as $2\Delta t, 4\Delta t, 8\Delta t$ etc., we rerun the program and measure the difference with the reference solution to confirm the second-order accuracy in terms of Δt for Example I. The numerical errors are shown in Table 1, which suggest the method is convergent and spectrally accurate in terms of Δt. Similarly, to test the spatial convergence, using a very small $\Delta\theta$, we take the solution as the reference solution. Then using large spatial steps such as $2\Delta\theta, 4\Delta\theta, 8\Delta\theta$ etc., we rerun the program and compare the solutions with the reference solution to obtain the error estimates (Table 2) which demonstrate the spectral accuracy in terms of $\Delta\theta$ for Example I.

$\widetilde{\sigma} > 0$ is a threshold concentration of nutrients needed for sustainability and μ is a parameter expressing the intensity of the expansion by mitosis (if $\sigma > \widetilde{\sigma}$) or shrinkage by apoptosis (if $\sigma < \widetilde{\sigma}$) within the tumor. Tumor grows corresponding to the normal velocity $v_n > 0$ and small $\widetilde{\sigma} \in (0, 1)$. Tumor shrinks corresponding to the normal velocities $v_n < 0$ and big $\widetilde{\sigma} \in (0, 1)$. The growth does not occur correspond to with $v_n = 0$. We take $\varepsilon(0) = 0$, growth and shrinkage cases are shown in Figure 1 (Left: $R(0) = 1, \mu = 5.2,\ \widetilde{\sigma} = 0.37$; Right: $R(0) = 12, \mu = 0.7,\ \widetilde{\sigma} = 0.6$), in which time is labeled.

When $\frac{d}{dt}(\frac{\varepsilon(t)}{R(t)}) = 0$, the tumor shape does not change in time and the evolution is linearly self-similar. This condition divides regimes of stable ($\frac{\varepsilon(t)}{R(t)} \to 0$) and unstable ($\left|\frac{\varepsilon(t)}{R(t)}\right| \to \infty$) growth.

For $\frac{d}{dt}(\frac{\varepsilon(t)}{R(t)}) = 0$, the shape of growing (or shrinking) tumor tends to become self-similar thereby preventing the occurrence of instabilities and invasive fingering. In Figure 2, self-similar (shape invariant) evolution is shown for different inital perturbation amplitudes $\frac{\varepsilon(0)}{R(0)} = 0$ and $\frac{\varepsilon(0)}{R(0)} = 0.38$.

For $\left|\frac{\varepsilon(t)}{R(t)}\right| \to \infty$, the perturbation grows unbounded with respect to unperturbed radius. For $\frac{\varepsilon(t)}{R(t)} \to 0$, the perturbation decays to zero. An initial small perturbation and the evolution of the perturbation during tumor growth are also considered. The perturbation may either grow or decay. In Figure 3, the growth of a perturbed circular initial boundary $r(\theta, 0) = 1.0 + 0.02cos(70\theta)$ is presented, in which $\mu = 5.2,\ \widetilde{\sigma} = 0.37$. Figure 3 indicates that the perturbation decays over time during tumor growth.

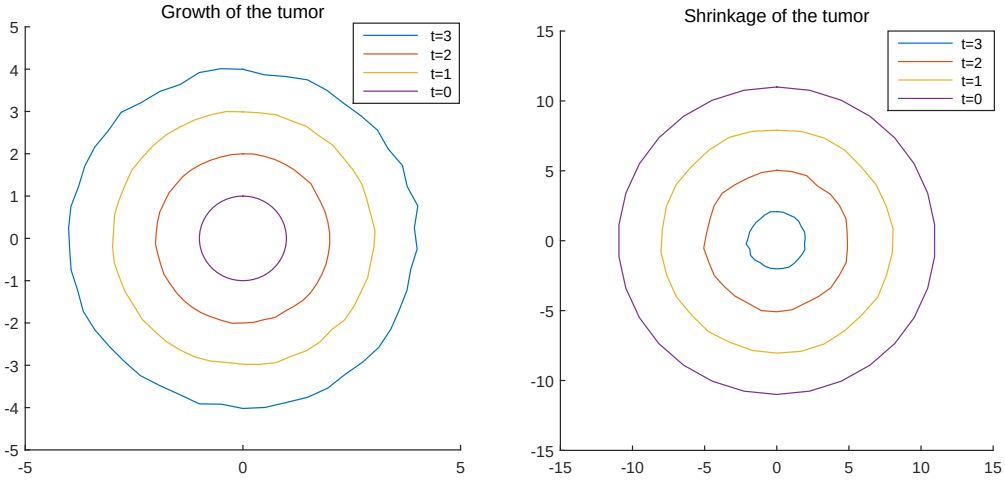

Figure 1: Left: the tumor grows rapidly due to normal velocity $v_n > 0$ ($\mu = 5.2,\ \widetilde{\sigma} = 0.37$, initial boundary $r = 1, \varepsilon = 0$). Right: the tumor shrinks rapidly due to normal velocity $v_n < 0$ ($\mu = 0.7,\ \widetilde{\sigma} = 0.6$, initial boundary $r = 12, \varepsilon = 0$).

Table 1 The difference between the numerical solutions and the reference solution confirms the second-order accuracy in terms of Δt for Example I.

Δt	$\|\|\| \sigma - \sigma_k^m \|\|\|_{\infty,0}$	$rate$	$\|\|\| p - p_k^m \|\|\|_{\infty,0}$	$rate$	$\|\|\| \frac{\partial p}{\partial n} - (\frac{\partial p}{\partial n})_k^m \|\|\|_{\infty,0}$	$rate$
0.008	9.779e-7	–	9.885e-7	–	9.982e-7	–
0.004	2.300e-7	2.0881	2.432e-7	2.0230	2.467e-7	2.0166
0.002	5.381e-8	2.0957	6.026e-8	2.0129	6.112e-8	2.0130
0.001	1.216e-8	2.1457	1.402e-8	2.1037	1.413e-8	2.1129

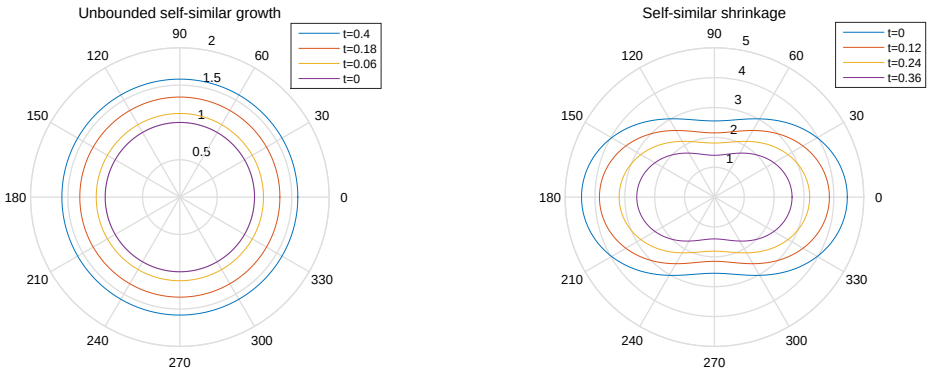

Figure 2: Left ($\varepsilon(0) = 0, R(0) = 1, 2n = 200$): During tumor growth, the tumor remains circular. Right ($\varepsilon(0) = 0.95, R(0) = 2.5, l = 2, 2n = 200$): During tumor shrinkage, analogous shapes are found to hold.

Table 2 The difference between the numerical solutions and the reference solution confirms the second-order accuracy in terms of $\Delta\theta$ for Example I.

$N = \frac{2\pi}{\Delta\theta}$	$\|\|\| \sigma - \sigma_k^m \|\|\|_{\infty,0}$	$rate$	$\|\|\| p - p_k^m \|\|\|_{\infty,0}$	$rate$	$\|\|\| \frac{\partial p}{\partial n} - (\frac{\partial p}{\partial n})_k^m \|\|\|_{\infty,0}$	$rate$
60	8.872e-7	–	8.916e-7	–	8.991e-7	–
120	2.217e-7	2.0007	2.229e-7	2.0000	2.248e-7	1.9998
240	5.501e-8	2.0108	5.513e-8	2.0155	5.602e-8	2.0046
480	1.327e-8	2.0515	1.358e-8	2.0214	1.381e-8	2.0202

7. Conclusions

In this work, we successfully apply Nystrom method based on trigonometric interpolatory quadratures for logarithmic singularities to free boundary problems (2.2) in R^2. However, this approach can't be extended to three-dimensional case because the square root singularities in R^3 cannot be split in the same way. It is possible to use the technique in R^3 for rotationally symmetric boundaries. [17]

In a future work, we plan to prove the convergences of boundary element method for free boundary problems, which have always been numerically tested, but, were rarely proven before in this field because the methods for fixed boundary are not applicable in free boundary problems.

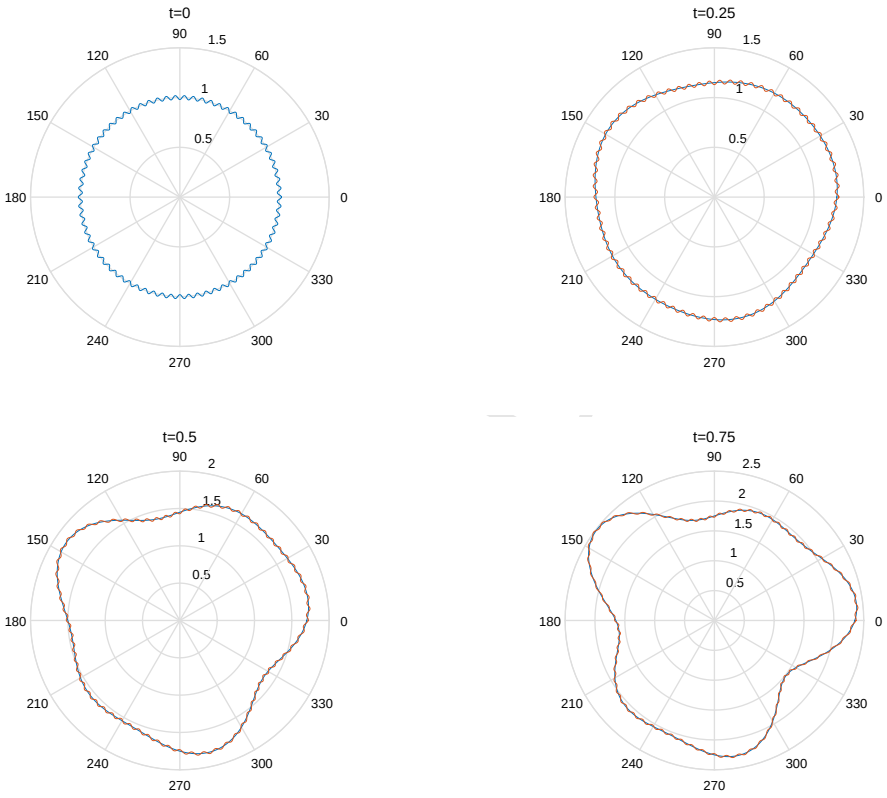

Figure 3: The evolution of a perturbed circular boundary with initial shape $r(\theta, 0) = 1.0 + 0.02cos(70\theta)$ indicates that the perturbation decays over time during tumor growth. Here $\mu = 5.2$, $\widetilde{\sigma} = 0.37$.

Acknowledgement

1. We would like to express our thanks to the editor and the reviewers whose valuable comments and suggestions brought us to spectral accuracy and helped to greatly improve this article.

2. We would like to thank Professor Bei Hu, who proposed the main idea.

References

[1] B. Hu, Blow-up theories for semi-linear parabolic equaitons, *Sprnger*, (2011).

[2] W. Hao, J. D. Hauenstein, B. Hu and A. J. Sommese, A three-dimensional steady-state tumor system, *Applied Mathematics and Computation*, Vol. 218, pp. 2661–2669, (2011).

[3] W. Hao, J. D. Hauenstein, B. Hu, Y. Liu, A. J. Sommese and Y. T. Zhang, Bifurcation for a free boundary problem modeling the growth of a tumor with a necrotic core, *Nonlinear Analysis Series B: Real World Applications*, Vol. 13, pp. 694–709, (2012).

[4] W. Hao, J. D. Hauenstein, B. Hu, Y. Liu, A. J. Sommese and Y.T. Zhang, Continuation along bifurcation branches for a tumor model with a necrotic core, *Journal of Scientific Computing*, Vol. 53, pp. 395–413, (2012).

[5] W. Hao, J. D. Hauenstein, B. Hu, T. McCoy and A. J. Sommese, Computing steady-state solutions for a free boundary problem modeling tumor growth by Stokes equation, *Journal of Computational and Applied Mathematics*, Vol. 237, pp. 326–334, (2013).

[6] W. Hao, J. D. Hauenstein, B. Hu and A. J. Sommese, A bootstrapping approach for computing multiple solutions of differential equations, *Journal of Computational and Applied Mathematics*, Vol. 258, pp. 181–190, (2014).

[7] W. Hao, B. Hu and A. J. Sommese, Cell cycle control and bifurcation for a free boundary problem modeling tissue growth, *Journal of Scientific Computing*, Vol. 56, pp. 350–365, (2013).

[8] A. Friedman, Variational Principles and Free Boundary Problems, *Wiley-Interscience Publication*, Wiley, New York, 1982.

[9] A. Friedman and B. Hu, A stefan problem for a protocell model, *Society for industrial and applied mathematics*, Vol. 30, pp 912–926, (1999).

[10] P.K. Banerjee, The Boundary Element Methods in Engineering, *McGraw-Hill, New York*, (1994).

[11] L. Morgado and P. Lima, Numerical solution of a class of singular free boundary problems involving the m-Laplace operator, *Journal*

of Computational and Applied Mathematics, Vol.234, pp. 2838–2847, (2010).

[12] J. P. Li, W. Chen, Z.J. Fu and L. l. Sun, Explicit empirical formula evaluating original intensity factors of singular boundary method for potential and Helmholtz problems, *Engineering Analysis with Boundary Elements*, Vol. 73, pp. 161–169, (2016).

[13] P. M. Lima and M. L. Morgado, Efficient computational methods for singular free boundary problems using smoothing variable substitutions, *Journal of Computational and Applied Mathematics*, Vol. 236, pp. 2981–2989, (2012).

[14] X. Sun and X. Li, A spectrally accurate boundary integral method for interfacial velocities in two-dimensional Stokes flow, *Commun. Comput. Phys.* , Vol. 8, pp. 933–946, (2010).

[15] S. Li and X. Li, A boundary integral method for computing the dynamics of an epitaxial island, *SIAM Journal on Scientific Computing*, Vol. 33, pp. 3282-3302, (2011).

[16] V. Cristini, J. Lowengrub and Q. Nie, Nonlinear simulation of tumor growth, *J. Math. Biol.* Vol. 46, pp. 191-224, (2003).

[17] R. Kress, Linear integral equations, *Springer- verlag*, (1989).

[18] P. Dimitrakoloupos and J. Wang, A spectral boundary element algorithm for interfacial dynamics in two-dimensional Stokes flow based on Hermitian interfacial smoothing, *Engng. Analy. Bound. Elem.* Vol. 31, pp. 646-656, (2007).

[19] M. C. Kropinski, An efficient numerical method for studying interfacial motion in twodimensional creeping flows, *J. Comput. Phys.*, Vol.171, pp. 479–508, (2001).